Eur J Nucl Med Mol Imaging
DOI 10.1007/s00259-016-3603-2

ORIGINAL ARTICLE

Myocardial blood flow and left ventricular functional reserve in hypertrophic cardiomyopathy: a $^{13}NH_3$ gated PET study

Roberto Sciagrà[1] · Raffaella Calabretta[1] · Fabrizio Cipollini[2] · Alessandro Passeri[1] · Angelo Castello[1] · Franco Cecchi[3] · Iacopo Olivotto[3] · Alberto Pupi[1]

Received: 5 September 2016 / Accepted: 16 December 2016

Abstract
Introduction Ischemia in hypertrophic cardiomyopathy (HCM) is caused by coronary microvascular dysfunction (CMD), which is detected by measuring myocardial blood flow (MBF) with PET. Whether CMD may be associated with ischemic left ventricular (LV) dysfunction is unclear. We therefore assessed LV ejection fraction (EF) reserve in HCM patients undergoing dipyridamole (Dip) PET.
Methods Resting and stress $^{13}NH_3$ dynamic as well as gated PET were performed in 34 HCM patients. Segmental MBF and transmural perfusion gradient (TPG = subendocardial / subepicardial MBF) were assessed. LVEF reserve was considered abnormal if Dip LVEF decreased more than 5 units as compared to rest.
Results Eighteen patients had preserved (group A) and 16 abnormal LVEF reserve (group B; range −7 to −32). Group B patients had greater wall thickness than group A, but resting volumes, LVEF, resting and Dip MBF, and myocardial flow reserve were similar. Group B had slightly higher summed stress score and summed difference score in visual analysis than group A, and a significantly higher summed stress wall motion score. In group B, resting TPG was slightly lower (1.31 ± 0.29 vs. 1.37 ± 0.34, $p < 0.05$), and further decreased after Dip, whilst in group A it increased ($B = 1.20 \pm 0.39$, $p < 0.0001$ vs. rest and vs. $A = 1.40 \pm 0.43$). The number of segments per patient with TPG <1 was higher than in group A ($p < 0.001$) and was a significant predictor of impaired LVEF reserve (OR 1.86, $p < 0.02$), together with wall thickness (OR 1.3, $p < 0.02$).
Conclusion Abnormal LVEF response is common in HCM patients following Dip, and is related to abnormal TPG, suggesting that subendocardial ischemia might occur under Dip and cause transient LV dysfunction. Although in vivo this effect may be hindered by the adrenergic drive associated with effort, these findings may have relevance in understanding exercise limitation and heart failure symptoms in HCM.

Keywords Hypertrophic Cardiomyopathy · Left Ventricular Ejection Fraction · Myocardial Blood Flow · N-13-Ammonia · Positron Emission Tomography

Introduction

Patients with hypertrophic cardiomyopathy (HCM) frequently report chest pain, and even typical anginal symptoms, but epicardial coronary artery disease is an exceptional finding [1–4]. Various studies indicate that a sizable proportion of HCM patients have stress induced perfusion defects as well as functional abnormalities, which can be of ischemic origin [1, 3–8]. Coronary microvascular dysfunction (CMD) is a major contributing mechanism for ischemia in HCM, and has major prognostic implications as well [4, 9–13]. Quantitative myocardial perfusion positron emission tomography (PET) represents an established and effective tool for measuring myocardial blood flow (MBF) and assessing CMD [14]. More recently, gated perfusion PET is gaining acceptance as a reliable approach to identify stress-induced functional abnormalities caused by ischemia in coronary artery

✉ Roberto Sciagrà
roberto.sciagra@unifi.it

[1] Nuclear Medicine Unit, Department of Experimental and Clinical Biomedical Sciences "Mario Serio", University of Florence, Largo Brambilla 3, 50134 Florence, Italy

[2] Department of Statistics, University of Florence, Florence, Italy

[3] Referral Centre for Myocardial Diseases, Careggi University Hospital, Florence, Italy

Published online: 03 January 2017

disease patients [15–18]. Thus, we found it interesting to examine the relationship between changes in left ventricular (LV) function and volumes as assessed by gated PET and quantitative myocardial perfusion PET parameters (MBF and myocardial flow reserve – MFR). Furthermore, prior studies have suggested that in HCM patients ischemia could specifically affect the subendocardium [19–27]. Therefore, we also focused our attention on the modifications in the MBF distribution within the myocardial wall, which the advances in quantitative PET techniques make possible to recognize [24, 27].

Materials and methods

Patient population

The study enrolled 34 patients with an established diagnosis of HCM (20 men and 14 women, mean age 49 ± 19, range 15 – 79 years) consecutively referred for cardiac PET to assess microvascular function, as part of a comprehensive clinical evaluation at the Florence Referral Centre for Cardiomyopathies. Partial data of 11 patients were reported in a previous study [27]. The diagnosis of HCM was based on evidence of a hypertrophied LV with maximal wall thickness ≥15 mm, in the absence of other cardiac or systemic causes explaining the degree of hypertrophy. To this aim, patients underwent comprehensive echocardiographic evaluation, which also defined the site and extent of maximal wall thickness, assessed at end-diastole. Moreover, by means of Doppler echocardiography, peak instantaneous outflow gradient was measured at baseline conditions [28]. In most patients, HCM diagnosis was confirmed by genetic analysis [29, 30]. Coronary artery disease had been excluded at the time of enrolment by maximal exercise tests in patients with low pre-test probability, followed by computed tomography (CT) angiography in case of uncertain or positive test results, and directly by CT angiography in patients with typical angina or high risk profile [31]. Table 1 summarizes the main features of the patient population. Our Ethics Committee approved the study, and all subjects signed a written informed consent form.

PET imaging

Patients were studied using our standard resting and stress protocol using a PET/CT Gemini TF scanner (Philips) [27]. After pharmacologic washout of five half-lives with the exception of amiodarone, avoidance of caffeine-containing beverages for 24 hours, and overnight fasting, patients were submitted to CT imaging for attenuation correction, followed by a resting study with administration of 370 MBq of $^{13}NH_3$ in slow bolus and dynamic list mode acquisition lasting 9 min. Immediately thereafter, an 8-frame gated PET acquisition was started for an additional 5 min. After 60 minutes, the stress study was performed using similar modalities, with the administration of 0.56 mg/kg of dipyridamole over 4 min. Patients were constantly monitored with automatic blood pressure measurements at 1-minute intervals and 12-lead electrocardiography. After 3 min of dipyridamole completion, 370 Mbq of $^{13}NH_3$ was injected and a second dynamic study acquired, again followed by a gated PET acquisition. Dynamic PET studies were then reconstructed with attenuation correction

Table 1 Baseline patient characteristics

	All patients	Group A	Group B	*p*
Gender (males/females)	20/14	13/5	7/9	NS
Age (years)	49 ± 19	55.8 ± 17.2	41.4 ± 17.7	<0.05
Smoker/smoking habit	11/34	6/18	5/16	NS
Hypertension	10/34	8/18	2/16	NS
Dyslipidemia	8/34	4/18	4/16	NS
Diabetes	2/34	1/18	1/16	NS
NYHA class > 1	19/34	8/18	11/16	NS
Angina	5/34	3/18	2/16	NS
Beta-blocking therapy (yes/no)	28/34	14/18	14/16	NS
Echocardiography				
LA diameter (mm)	43 ± 8	44 ± 9	43 ± 8	NS
LV maximal thickness (mm)	22 ± 6	19 ± 4	25 ± 6	<0.0001
LV ED diameter (mm)	44 ± 7	47 ± 6	40 ± 7	<0.005
LV Ejection Fraction (%)	66 ± 9	66.5 ± 10	66 ± 7	NS
LV OTG (mmHG)	21 ± 25	18 ± 20	24 ± 30	NS
Obstructive at rest (LVOTG ≥ 30 mmHG)	8/34	4/18	4/16	NS

Abbreviations. ED = end-diastolic; ES = end-systolic; LA = left atrium; LV = left ventricle; NS = not significant, NYHA = New York Heart Association; OTG = outflow tract gradient (measured by Doppler echocardiography).

using a BLOB-OS-TF iterative algorithm with 33 subsets, three iterations, relaxation parameter = 1, on 144 x 144 x 45 matrices. The dynamic list sequence was reframed for off-line quantitative MBF measurement in a dynamic series of 24 frames of 5 sec, two of 30 sec, and one of 60 sec duration, followed by a prolonged frame for the next 5 min. We did not apply electrocardiographic or respiratory gating. The gated PET acquisition was reconstructed using the iterative method 3D-RAMLA (45 slices, matrix 144x144, voxel dimensions: 4x4x4mm) with two iterations and three subsets, after decay, attenuation, random, scatter and time of flight correction. Before the final reconstruction of both the dynamic and gated images, the alignment of CT and PET images was controlled and corrected if necessary.

Qualitative perfusion assessment

Resting and stress $^{13}NH_3$ uptake on the summed gated images was visually rated by an experienced observer, blind to the other patient data, using a 5-point scale on the AHA 17-segment model and the results expressed as summed rest score (SRS), summed stress score (SSS) and summed difference score (SDS) [32, 33].

MBF quantification

The reconstructed images were transferred to a workstation for quantification using the PMOD platform (PMOD Technologies, version 3.607). A preliminary evaluation of possible movement artefacts in the dynamic frame sequence was performed and correction of the abnormal frames was performed using the PFUS tool. Then, using the semiautomatic interactive procedure of the PCARD tool, the images were reoriented along the heart axis, and segmented into the 17 AHA segments within the detected endo- and epicardial borders [33]. For each myocardial segment, the average time-activity curve (TAC) of tracer concentration was calculated using the first 240 sec of the dynamic acquisition. VOIs were generated in the LV and in the right (R) ventricle to obtain the blood activity TACs. An arterial input function (AIF) was derived from the LV TAC by applying a linear metabolite correction according to DeGrado et al. [34]. The segmental MBF values were obtained by fitting a single-tissue compartment model [34] with spillover from LV and RV to the respective myocardial TACs. The segmental values were averaged using a volume-weighted procedure to derive the global LV MBF. Moreover, using a volume-weighted procedure and the standard segment attribution, the segmental values were averaged to derive the MBF of the three coronary artery territories: left anterior descending (LAD), left circumflex (LCX) and right coronary artery (RCA). MFR was calculated as Dip-MBF / resting MBF. As part of the fitting process, a parametric MBF map was also generated within the endo- and epicardial boundaries [35]. The procedure used the same AIF, dual spill-over correction and single-tissue compartment model, but fitted the pixelwise TACs using a basis function approach as previously described [27].

Transmural Layer analysis

The procedure has been already described [27]. Briefly, a segmented mask was created and superimposed on the parametric perfusion map. Then, the MBF values of the pixels assigned to each segment were exported in a matrix file together with their orthogonal coordinates. Using these coordinates and having as reference the center of the LV cavity, the pixels and their MBF values were rearranged in different layers starting from the innermost. If more than two layers were obtained, their total number was finally divided by two, the internal half was summed to build the subendocardial and the external half to build the subepicardial layer. Once the subendocardial and subepicardial layers were identified, the MBF of each segment was computed by averaging the values of the pixels belonging to it. For the whole procedure, we used ad-hoc programmed functions in the R environment [36]. The obtained values were used to calculate separately the subepicardial and subendocardial MBF and the transmural perfusion gradient (TPG), which was defined as subendocardial MBF / subepicardial MBF. As a threshold for classifying a segment as possibly affected by subendocardial ischemia, we considered a Dip TPG < 1.

Gated PET evaluation

A visual analysis of LV regional wall motion was performed by an experienced observer blind to the other patient data, and the results were reported using the 17-segment model and a 6-point scoring scale to derive the summed rest score for wall motion (SRSWM) and the summed stress score for wall motion (SSSWM) [37]. Rest and Dip-LV end-diastolic (ED) and end-systolic (ES) volumes (V) and EF were calculated using commercially available software (Emory Cardiac Tool Box; Emory University Hospital) [15, 18]. Volumes were expressed as indexes (i), by dividing them by the body surface area. The LVEF reserve was computed as Dip LVEF minus rest LVEF. Because of the lack of a specific threshold for defining the stress gated PET LVEF with $^{3}NH_3$ as abnormal, we used the restrictive cut off of a drop larger than – 5 LVEF units, currently used for gated SPECT, instead of adopting the absence of increase as some proposed for ^{82}Rb gated PET [15–18, 38, 39].

Statistical analysis

Variables are expressed as mean ± standard deviation or as median (interquartile range) as appropriate. The comparison within and between groups was performed with the Student's t

test for paired or unpaired samples, or the Mann–Whitney nonparametric test, as appropriate. The comparison of proportion was performed with the Fisher's exact test. Correlation between LVEF reserve and number of abnormal segments in PET was evaluated using linear regression. Stepwise binary logistic analysis was used to identify the significant predictors of abnormal LVEF reserve and to calculate the odds ratio (OR) and its 95% confidence interval (CI). A $p < 0.05$ was required for statistical significance. All analyses were performed using SPSS, version 22.0.

Results

Gated PET

At resting gated PET, EDVi was 63 ± 21 mL and ESVi 28 ± 16 mL, with LVEF 58 ± 10%. At maximal vasodilation, EDVi was 75 ± 26 mL and ESVi 37 ± 24 mL, with EF 54 ± 15%. LVEF reserve for the whole cohort was −3.8 ± 11%. In particular, there were 18 patients with preserved LVEF reserve, ranging from +17 to −5%, (= group A) and 16 patients with impaired LVEF reserve as above defined, ranging from −7 to −32% (group B). Figures 1 and 2 show examples of patients in the two groups. As compared to group A, group B patients were younger, had greater LV wall thickness and smaller LV end-diastolic diameter. Table 2 compares patient haemodynamics at rest and during dipyridamole stress. At rest the two groups had similar LV volume indexes and EF; after stress, group B patients had significantly larger ESVi (48 ± 27 vs. 26 ± 15mL, $p < 0.01$). The SRSWM of the two groups did not differ; conversely, group B had a significantly higher SSSWM than group A: 3 (2.25 – 5) vs. 0 (0 – 0.25), $p < 0.0001$.

Qualitative perfusion assessment

The SRS was not significantly different between the two groups: A = 0 (0 – 1.25) vs. B = 1 (0 – 2), NS. A borderline difference was registered for SSS and SDS: A = 2 (0 – 3.25) vs. B = 3.5 (2 – 6.75), $p < 0.05$, and A = 0.5 (0 – 2) vs. B = 2 (1 – 5.75), $p < 0.05$, respectively.

Average wall MBF

Global resting MBF was 0.86 ± 0.20 mL/min/g in group A and 0.89 ± 0.18 mL/min/g in group B (NS). Dip MBF was 1.86 ± 0.41 mL/min/g vs.1.93 ± 0.56 mL/min/g, respectively

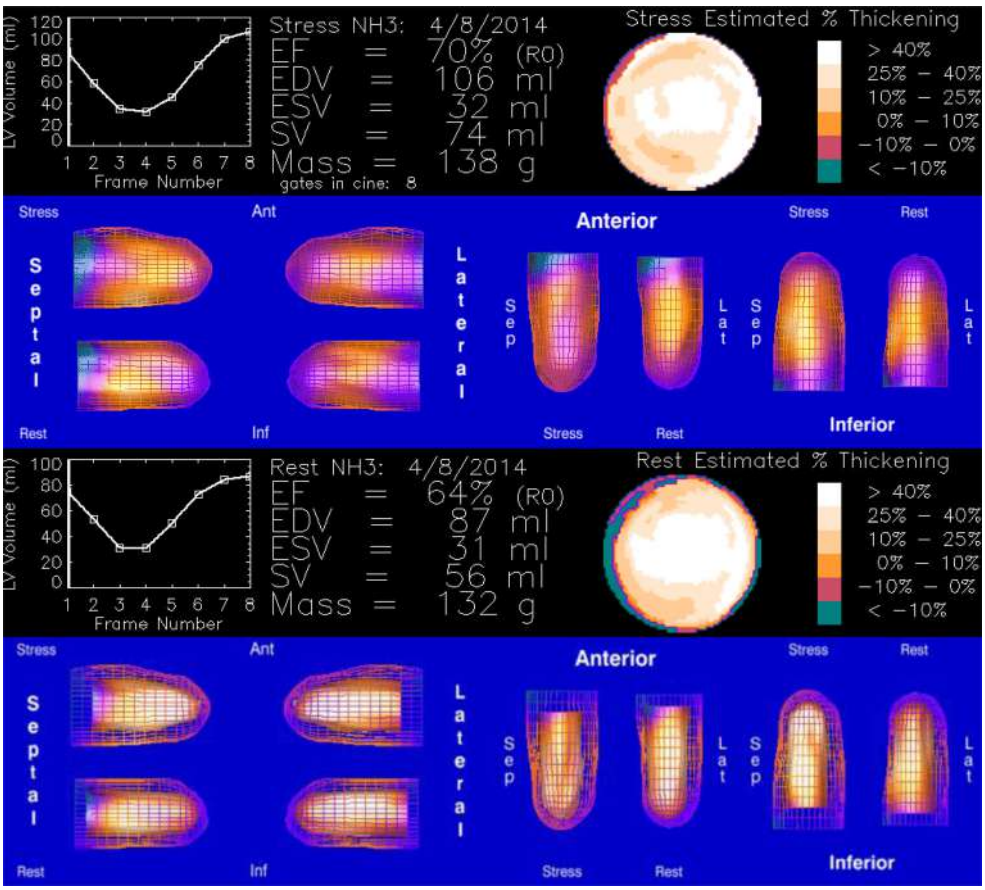

Fig. 1 Results of gated PET analysis in a patient of group A. Rows from top to bottom: first and third row: LV volume curve and LV volumes after stress and at rest respectively; second and fourth row: frozen three-dimensional images after stress and at rest at end-diastole and end-systole, respectively. The normal response to stress is shown

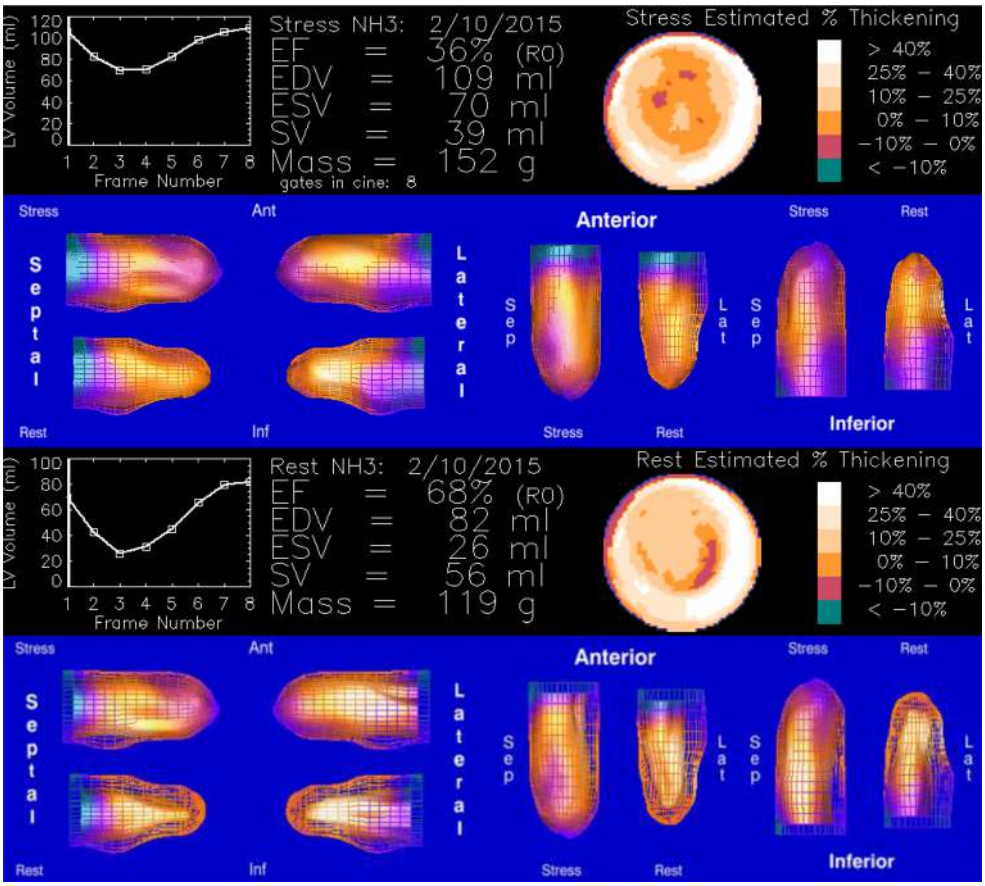

Fig. 2 Results of gated PET analysis in a patient of group B. Same image disposition as in Fig 1. The clear LVEF decrease and LV volumes increase after stress are both apparent

(NS) and MFR was 2.3 ± 0.9 vs. 2.2 ± 0.7, respectively (NS). Table 3 reports the resting and Dip MBF and the MFR of the three coronary artery territories, which do not show significant differences between the two groups. The number of segments per patient with Dip MBF in the lowest quartile (<1.50 mL/min/g) was not different: 1 (0 – 9.75) in group A patients and 4 (0 – 7) in group B (NS). Similarly, the number of segments per patient with MFR < 2 was comparable: 4 (0 – 15) in group A patients and 10 (1 – 14.75) in group B (NS).

Transmural analysis

Table 4 shows the subendocardial and subepicardial segmental MBF values in the two patients groups. At rest, group B patients had higher MBF in both layers than group A, whilst their resting TPG was just borderline lower. Following Dip, both groups reached a similar level of subendocardial MBF, whilst the subepicardial MBF remained significantly higher in group B than in group A. As a consequence, the Dip TPG of group B patients decreased considerably as compared to the

Table 2 Hemodynamics at baseline and under dipyridamole stress

	Group A		*p*	Group B		*p*
	Baseline	Dipyridamole		Baseline	Dipyridamole	
Heart rate (beats/min)	62 ± 10	83 ± 12	<0.0001	58 ± 8	86 ± 14	<0.0001
Systolic BP (mmHg)	128 ± 25	123 ± 22	NS	114 ± 25	114 ± 26	NS
Diastolic BP (mmHg)	63 ± 13	61 ± 16	NS	59 ± 16	59 ± 17	NS
RPP	7946 ± 2128	10100 ± 1642	<0.0001	6816 ± 2216	9989 ± 3671	<0.0001

Abbreviations. BP = blood pressure; RPP = rate pressure product.

Table 3 Resting and Dip-MBF and MFR in the three coronary artery territories

	Resting MBF (mL/min/g)		*p*	Dip-MBF (mL/min/g)		*p*	MFR		*p*
	Group A	Group B		Group A	Group B		Group A	Group B	
LAD	0.86 ± 0.22	0.90 ± 0.18	NS	1.79 ± 0.41	1.87 ± 0.53	NS	2.23 ± 0.90	2.13 ± 0.68	NS
LCX	0.86 ± 0.21	0.90 ± 0.18	NS	1.99 ± 0.40	2.09 ± 0.62	NS	2.49 ± 0.99	2.40 ± 0.77	NS
RCA	0.87 ± 0.21	0.87 ± 0.16	NS	1.83 ± 0.46	1.87 ± 0.58	NS	2.24 ± 0.91	2.21 ± 0.72	NS

Abbreviations. Dip = dipyridamole; LAD = left anterior descending; LCX = left circumflex artery; MBF = myocardial blood flow; MFR = myocardial flow reserve; RCA = right coronary artery.

corresponding resting value, and became very significantly lower than that in group A (Fig. 3). The number of segments per patient with Dip TPG < 1 was 3 (1 – 3.25) in group A and 5.5 (4 – 7.75) in group B ($p < 0.001$).

Predictors of abnormal LVEF response

The drop in LVEF between Dip and rest had just a borderline correlation with SSS ($r = -0.3$, $p < 0.05$, $R^2 = -0.15$, $p < 0.05$) and with SDS ($r = -0.43$, $p < 0.01$, $R^2 = -0.19$, $p < 0.01$). On the other hand, the difference in LVEF correlated significantly with the number of segments per patient with Dip TPG < 1 ($r = -0.6$, $p < 0.0001$, $R^2 = -0.34$, $p < 0.0001$) (Fig. 4), but not with number of segments with Dip MBF in the lowest quartile or with MFR <2. The following variables showing a significant difference between the two groups of patients were included in the stepwise binary logistic analysis: age, LV wall thickness, LV end-diastolic diameter, SSS, SDS, SSSWM, and number of segments per patient with TPG < 1. According to the logistic analysis, the maximal LV wall thickness (OR 1.3, 95% CI 1.05 – 1.53, $p < 0.02$) and the number of segments per patient with Dip TPG < 1 (OR 1.86, 95% CI 1.12 – 3.08, $p < 0.02$) were significant predictors of abnormal LVEF reserve. According to the predictive model, 28 patients (82%) could be correctly classified as belonging to the group with normal or that with abnormal LVEF response.

Discussion

In this study we detected in a high proportion of HCM patients an abnormal response under Dip, characterized by a significant drop in LVEF associated with regional wall motion abnormalities, and slightly reduced stress tracer uptake, but not with differences in transmural MBF or MFR. On the other hand, these patients show significantly more severe signs suggestive of possible subendocardial ischemia as compared to the remaining patients with preserved stress LVEF. These results are in agreement with two recent reports dealing with the relationship between MBF and functional changes in HCM patients [26, 40]. In 33 subjects, Bravo et al. showed a trend towards LVEF decrease after stress, which appeared to be greater in those with obstructive disease [40]. More recently, they demonstrated the occurrence of transient ischemic LV dilation in more than one half of 61 HCM patients [26]. Collectively, these data confirm earlier observations showing LVEF decrease and regional wall motion changes during dobutamine stress or exercise stress testing in a sizable proportion of HCM patients [7, 8]. However, the main advantage of assessing function by means of (gated) PET is that this modality allows MBF quantification as well, and, therefore, permits exploring the relationship between functional markers of potential ischemia and abnormalities in myocardial perfusion. In particular, it is possible to assess under which conditions CMD causes true myocardial ischemia and which parameters influence its capability to impair myocardial contractility. Because of its design, the first study by Bravo et al. did not evaluate the relationship between MBF and LVEF response, but demonstrated that stress LVEF was, together with wall thickness, a predictor of impaired maximal MBF and MFR [40]. In the second study, the same group found that patients with LV dilation under stress had increased wall thickness and lower peak MBF, MFR and LVEF reserve [26]. This is consistent with the finding in our cohort, in whom maximal LV

Table 4 Subendocardial and subepicardial MBF in the two patient groups

	Group A		*p*	Group B		*p*
	Rest	Dipyridamole		Rest	Dipyridamole	
Subendocardial MBF (mL/min/g)	0.77 ± 0.19	1.50 ± 0.38	<0.0001	0.84 ± 0.19*	1.49 ± 0.49	<0.0001
Subepicardial MBF (mL/min/g)	0.60 ± 0.22	1.16 ± 0.44	<0.0001	0.67 ± 0.19*	1.34 ± 0.56*	<0.0001
TPG	1.37 ± 0.34	1.40 ± 0.43	NS	1.31 ± 0.29†	1.20 ± 0.39*	<0.0001

Abbreviations. TPG = transmural perfusion gradient. * = $p < 0.0001$ vs. group A; † = $p < 0.05$ vs. group A.

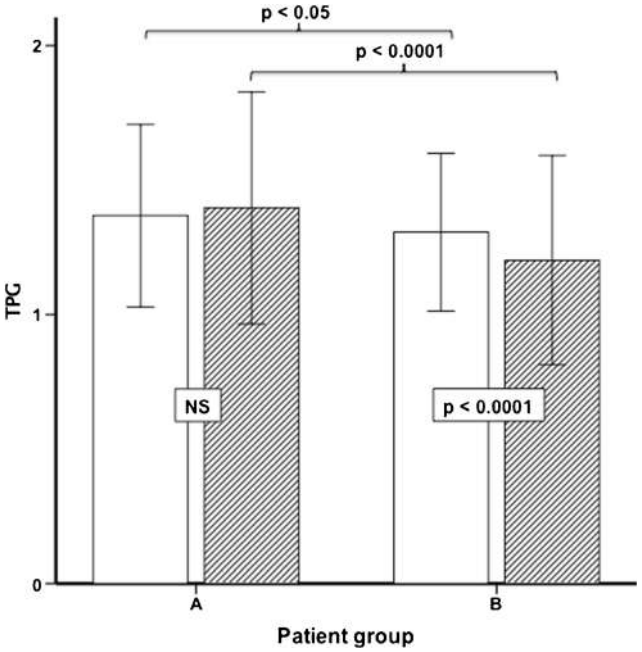

Fig. 3 Bar graph showing TPG at rest and during stress in the two patient groups

wall thickness is an independent predictor of LVEF reserve. However, we could not identify a significant difference in global or regional Dip MBF and MFR between the two groups. Also the number of segments per patient with either abnormality (Dip MBF in the lowest quartile or MFR <2) was not significantly different in the two groups, whilst the SSS and SDS were just borderline higher. Therefore, it appears reasonable to look for other factors leading to an abnormal and possibly ischemic LVEF response.

Our data suggest that isolated subendocardial ischemia might play a role in determining functional impairment in HCM patients during maximal coronary vasodilatation. Various prior reports had suggested that the distribution of ischemia in HCM patients could selectively involve the subendocardium, and that this phenomenon could be detected in terms of cavitation in myocardial perfusion SPECT [20, 21]. The limited resolution of perfusion SPECT and the lack of quantitative capabilities of that modality, however, precluded the definitive demonstration of true subendocardial ischemia. This was later achieved by means of magnetic resonance imaging with perfusion assessment and late gadolinium enhancement [22, 25]. More recently, however, also the quantification of MBF with PET has been able to identify abnormalities in subendocardial perfusion in HCM patients [24, 27]. According to our results, an inversion of the normal TPG that suggests an abnormal subendocardial Dip MBF can be detected in a large portion of HCM patients and appears much more frequent among those with an abnormal LVEF response. Interestingly, this finding was not accompanied by an overall worse Dip MBF in our series. This apparent disagreement with the results published by Bravo et al. [26] could be in part explained by the different characteristics of the patient

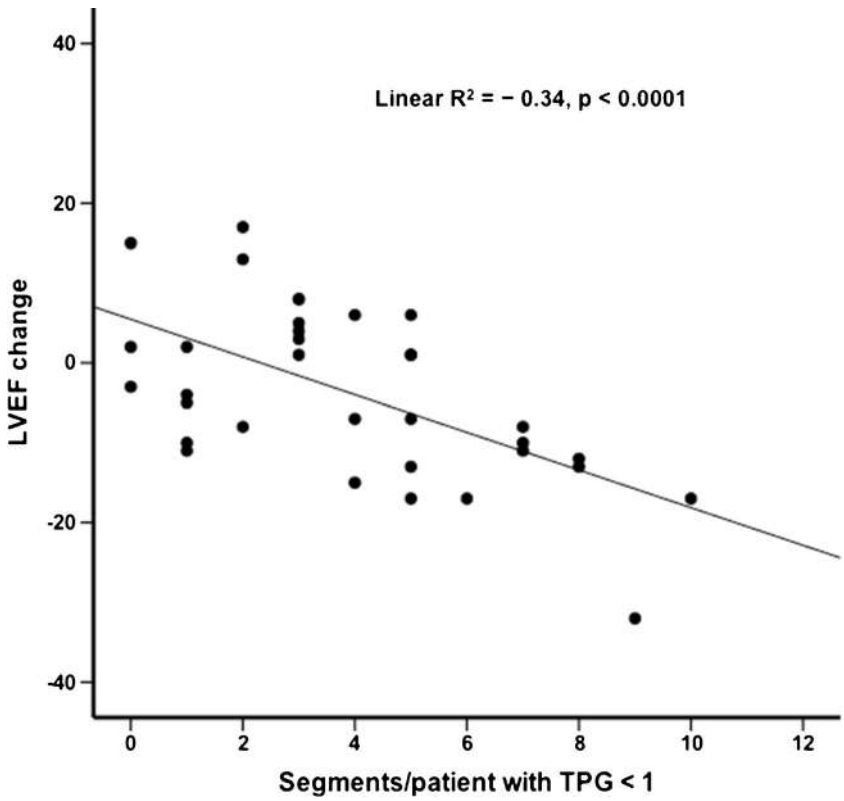

Fig. 4 Relationship between number of segments per patient with Dip TPG < 1 and the LVEF change (= stress – rest LVEF difference)

populations, with higher prevalence of patients with dynamic obstruction, hypertension and angina in their cohort as compared to ours. This could imply that in general those patients were more severely affected than ours, so that the phase of isolated subendocardial ischemia has been already overcome by the occurrence of overt transmural ischemia.

From a pathophysiological standpoint, the occurrence of ischemia at the subendocardial level in HCM makes sense, and was many years ago postulated to occur [4]. Small vessel disease is considered the morphologic substrate for the microvascular dysfunction, and several factors could enhance its effects on the subendocardium, increasing the likelihood of discrepancies between oxygen demand and oxygen supply [4]. Furthermore, classic studies using pacing and lactate titration in the coronary sinus had already demonstrated that HCM ischemia might occur despite an increase in coronary flow [41]. Recent reports demonstrate that in HCM patients various other mechanisms beyond supply/demand mismatch and remodelling of the intramyocardial blood vessels concur in causing ischemia during adenosine stimulation, such as increased microvascular resistances and derangements in coronary flow [42, 43]. On the other hand, a reduction in LVEF is not usually observed in HCM patients during physiological exercise – which generally elicits the expected inotropic response by the LV [28]. This apparent discrepancy with the present study might be explained by the adrenergic surge associated with exercise – which is not elicited during Dip – potentially overcoming the effect of abnormal perfusion on systolic function. This hypothesis, however, requires further investigation.

Various limitations of our study must be considered, first of all the small sample size. Since we used $^{13}NH_3$ as perfusion tracer, the acquisition of gated PET after stress was slightly delayed as compared to the standard ^{82}Rb protocols, and this could limit the capability to identify transient Dip-induced LVEF abnormalities [44]. On the other hand, we adopted a quite restrictive threshold for defining LVEF drop as significant: in ^{82}Rb gated PET the minus 5% in stress images is regarded as extremely specific for severe coronary artery disease, and this value is currently used in perfusion gated SPECT, where the delay in the post-stress acquisition is certainly more prolonged than that with $^{13}NH_3$ PET [38, 39]. We observed some degree of underestimation of LVEF with $^{13}NH_3$ PET as compared to echocardiography in both patient groups, a circumstance that should have not influenced the evaluation of stress-induced changes. Moreover, although previous data suggested a good correlation of $^{13}NH_3$ gated PET with other modalities, a most recent paper identifies a trend to underestimation of LVEF using $^{13}NH_3$ gated PET as compared to echocardiography [45, 46]. The limited resolution of PET images remains a major obstacle to the accurate definition of subendocardial and subepicardial MBF. With regard to this, our results are also affected by the lack of respiratory and cardiac gating. The latter limitation involves the whole dynamic acquisition on which the TACs for MBF quantification are calculated. Moreover, even the attenuation correction procedure could be a source of error, because of the misalignment between the frozen CT image and the moving heart in PET [47]. This is so far a common problem for all quantitative PET studies. Further technical improvements, such as gating of dynamic studies and implementation of more refined reconstruction protocols are highly desirable [48]. However, since the same approach was used in different patient groups with the same disease, these limitations should marginally affect the inter-group comparisons.

Conclusion

Abnormal LVEF response is common in HCM patients following dipyridamole infusion, and is related to impaired transmural perfusion gradient, suggesting that subendocardial ischemia occurs under stress and may cause transient LV dysfunction. Although in vivo this effect may be hindered by the adrenergic drive associated with effort, these findings may have relevance in understanding exercise limitation and heart failure symptoms in HCM.

Compliance with ethical standards

Funding sources This work was supported by the Italian Ministry of Health (RF 2010 – 2313451 and NET-2011-02347173).

Disclosures None.

Ethical approval All procedures performed in studies involving human participants were in accordance with the ethical standards of the institutional and/or national research committee and with the 1964 Helsinki Declaration and its later amendments or comparable ethical standards.

References

1. Pitcher D, Wainwright R, Maisey M, Curry P, Sowton E. Assessment of chest pain in hypertrophic cardiomyopathy using exercise thallium-201 myocardial scintigraphy. Br Heart J. 1980;44:650–6.
2. Elliott PM, Kaski JC, Prasad K, Seo H, Slade AK, Goldman JH, et al. Chest pain during daily life in patients with hypertrophic cardiomyopathy: an ambulatory electrocardiographic study. Eur Heart J. 1996;17:1056–64.
3. Maron BJ. Hypertrophic cardiomyopathy: a systematic review. JAMA. 2002;287:1308–20.
4. Maron MS, Olivotto I, Maron BJ, Prasad SK, Cecchi F, Udelson JE, et al. The case for myocardial ischemia in hypertrophic cardiomyopathy. J Am Coll Cardiol. 2009;54:866–75.
5. O'Gara PT, Bonow RO, Maron BJ, Damske BA, Van Lingen A, Bacharach SL, et al. Myocardial perfusion abnormalities in patients with hypertrophic cardiomyopathy: assessment with thallium-201 emission computed tomography. Circulation. 1987;76:1214–23.

6. Cannon 3rd RO, Dilsizian V, O'Gara PT, Udelson JE, Schenke WH, Quyyumi A, et al. Myocardial metabolic, hemodynamic, and electrocardiographic significance of reversible thallium-201 abnormalities in hypertrophic cardiomyopathy. Circulation. 1991;83:1660–7.
7. Okeie K, Shimizu M, Yoshio H, Ino H, Yamaguchi M, Matsuyama T, et al. Left ventricular systolic dysfunction during exercise and dobutamine stress in patients with hypertrophic cardiomyopathy. J Am Coll Cardiol. 2000;36:856–63.
8. Ciampi Q, Betocchi S, Losi MA, Ferro A, Cuocolo A, Lombardi R, et al. Abnormal blood-pressure response to exercise and oxygen consumption in patients with hypertrophic cardiomyopathy. J Nucl Cardiol. 2007;14:869–75.
9. Camici P, Chiriatti G, Lorenzoni R, Bellina RC, Gistri R, Italiani G, et al. Coronary vasodilation is impaired in both hypertrophied and nonhypertrophied myocardium of patients with hypertrophic cardiomyopathy: a study with nitrogen-13 ammonia and positron emission tomography. J Am Coll Cardiol. 1991;17:879–86.
10. Choudhury L, Rosen SD, Patel D, Nihoyannopoulos P, Camici PG. Coronary vasodilator reserve in primary and secondary left ventricular hypertrophy. A study with positron emission tomography. Eur Heart J. 1997;18:108–16.
11. Cecchi F, Olivotto I, Gistri R, Lorenzoni R, Chiriatti G, Camici PG. Coronary microvascular dysfunction and prognosis in hypertrophic cardiomyopathy. N Engl J Med. 2003;349:1027–35.
12. Olivotto I, Cecchi F, Gistri R, Lorenzoni R, Chiriatti G, Girolami F, et al. Relevance of coronary microvascular flow impairment to long-term remodeling and systolic dysfunction in hypertrophic cardiomyopathy. J Am Coll Cardiol. 2006;47:1043–8.
13. Cecchi F, Sgalambro A, Baldi M, Sotgia B, Antoniucci D, Camici PG, et al. Microvascular dysfunction, myocardial ischemia, and progression to heart failure in patients with hypertrophic cardiomyopathy. J Cardiovasc Transl Res. 2009;2:452–61.
14. Sciagrà R, Passeri A, Bucerius J, Verberne HJ, Slart RH, Lindner O, et al. Cardiovascular Committee of the European Association of Nuclear Medicine (EANM). Clinical use of quantitative cardiac perfusion PET: rationale, modalities and possible indications. Position paper of the Cardiovascular Committee of the European Association of Nuclear Medicine (EANM). Eur J Nucl Med Mol Imaging. 2016;43:1530–45.
15. Dorbala S, Vangala D, Sampson U, Limaye A, Kwong R, Di Carli MF. Value of vasodilator left ventricular ejection fraction reserve in evaluating the magnitude of myocardium at risk and the extent of angiographic coronary artery disease: a 82Rb PET/CT study. J Nucl Med. 2007;48:349–58.
16. Brown TL, Merrill J, Volokh L, Bengel FM. Determinants of the response of left ventricular ejection fraction to vasodilator stress in electrocardiographically gated (82)rubidium myocardial perfusion PET. Eur J Nucl Med Mol Imaging. 2008;35:336–42.
17. Dorbala S, Hachamovitch R, Curillova Z, Thomas D, Vangala D, Kwong RY, et al. Incremental prognostic value of gated Rb-82 positron emission tomography myocardial perfusion imaging over clinical variables and rest LVEF. JACC Cardiovasc Imaging. 2009;2:846–54.
18. Van Tosh A, Votaw JR, Reichek N, Palestro CJ, Nichols KJ. The relationship between ischemia-induced left ventricular dysfunction, coronary flow reserve, and coronary steal on regadenoson stress-gated (82)Rb PET myocardial perfusion imaging. J Nucl Cardiol. 2013;20:1060–8.
19. Choudhury L, Elliott P, Rimoldi O, Ryan M, Lammertsma AA, Boyd H, et al. Transmural myocardial blood flow distribution in hypertrophic cardiomyopathy and effect of treatment. Basic Res Cardiol. 1999;94:49–59.
20. Yoshida N, Ikeda H, Wada T, Matsumoto A, Maki S, Muro A, et al. Exercise-induced abnormal blood pressure responses are related to subendocardial ischemia in hypertrophic cardiomyopathy. J Am Coll Cardiol. 1998;32:1938–42.
21. Nakamura T, Sakamoto K, Yamano T, Kikkawa M, Zen K, Hikosaka T, et al. Increased plasma brain natriuretic peptide level as a guide for silent myocardial ischemia in patients with non-obstructive hypertrophic cardiomyopathy. J Am Coll Cardiol. 2002;39:1657–63.
22. Petersen SE, Jerosch-Herold M, Hudsmith LE, Robson MD, Francis JM, Doll HA, et al. Evidence for microvascular dysfunction in hypertrophic cardiomyopathy: new insights from multiparametric magnetic resonance imaging. Circulation. 2007;115:2418–25.
23. Kawasaki T, Sugihara H. Subendocardial ischemia in hypertrophic cardiomyopathy. J Cardiol. 2014;63:89–94.
24. Knaapen P, Germans T, Camici PG, Rimoldi OE, ten Cate FJ, ten Berg JM, et al. Determinants of coronary microvascular dysfunction in symptomatic hypertrophic cardiomyopathy. Am J Physiol Heart Circ Physiol. 2008;294:H986–993.
25. Ismail TF, Hsu LY, Greve AM, Gonçalves C, Jabbour A, Gulati A, et al. Coronary microvascular ischemia in hypertrophic cardiomyopathy - a pixel-wise quantitative cardiovascular magnetic resonance perfusion study. J Cardiovasc Magn Reson. 2014;16:49.
26. Bravo PE, Tahari A, Pozios I, Luo HC, Bengel FM, Wahl RL, et al. Apparent left ventricular cavity dilatation during PET/CT in hypertrophic cardiomyopathy: Clinical predictors and potential mechanisms. J Nucl Cardiol. 2015.
27. Sciagrà R, Passeri A, Cipollini F, Castagnoli H, Olivotto I, Burger C, et al. Validation of pixel-wise parametric mapping of myocardial blood flow with 13NH3 PET in patients with hypertrophic cardiomyopathy. Eur J Nucl Med Mol Imaging. 2015;42:1581–8.
28. Maron MS, Olivotto I, Zenovich AG, Link MS, Pandian NG, Kuvin JT, et al. Hypertrophic cardiomyopathy is predominantly a disease of left ventricular outflow tract obstruction. Circulation. 2006;114:2232–39.
29. Olivotto I, Cecchi F, Poggesi C, Yacoub MH. Patterns of disease progression in hypertrophic cardiomyopathy: an individualized approach to clinical staging. Circ Heart Fail. 2012;5:535–46.
30. Olivotto I, Girolami F, Ackerman MJ, Nistri S, Bos JM, Zachara E, et al. Myofilament protein gene mutation screening and outcome of patients with hypertrophic cardiomyopathy. Mayo Clin Proc. 2008;83:630–38.
31. Olivotto I, Girolami F, Sciagrà R, Ackerman MJ, Sotgia B, Bos JM, et al. Microvascular function is selectively impaired in patients with hypertrophic cardiomyopathy and sarcomere myofilament gene mutations. J Am Coll Cardiol. 2011;58:839–48.
32. Machac J, Bacharach SL, Bateman TM, Bax JJ, Beanlands R, Bengel F, et al. Quality Assurance Committee of the American Society of Nuclear Cardiology. Positron emission tomography myocardial perfusion and glucose metabolism imaging. J Nucl Cardiol. 2006;13:e121.
33. Cerqueira MD, Weissman NJ, Dilsizian V, Jacobs AK, Kaul S, Laskey WK, et al. American Heart Association Writing Group on Myocardial Segmentation and Registration for Cardiac Imaging. Standardized myocardial segmentation and nomenclature for tomographic imaging of the heart. Circulation. 2002;105:539–42.
34. DeGrado TR, Hanson MW, Turkington TG, Delong DM, Brezinski DA, Vallée JP, et al. Estimation of myocardial blood flow for longitudinal studies with 13N-labeled ammonia and positron emission tomography. J Nucl Cardiol. 1996;3:494–507.
35. Harms HJ, de Haan S, Knaapen P, Allaart CP, Lammertsma AA, Lubberink M. Parametric images of myocardial viability using a single 15O-H2O PET/CT scan. J Nucl Med. 2011;52:7459.
36. R Core Team (2014). R: A language and environment for statistical computing. R Foundation for Statistical Computing, Vienna, Austria. URL http://www.R-project.org/

37. Emmett L, Iwanochko RM, Freeman MR, Barolet A, Lee DS, Husain M. Reversible regional wall motion abnormalities on exercise technetium-99m-gated cardiac single photon emission computed tomography predict high-grade angiographic stenoses. J Am Coll Cardiol. 2002;39:991–8.
38. Hida S, Chikamori T, Tanaka H, Usui Y, Igarashi Y, Nagao T, et al. Diagnostic value of left ventricular function after stress and at rest in the detection of multivessel coronary artery disease as assessed by electrocardiogram-gated SPECT. J Nucl Cardiol. 2007;14:68–74.
39. Dona M, Massi L, Settimo L, Bartolini M, Giannì G, Pupi A, et al. Prognostic implications of post-stress ejection fraction decrease detected by gated SPECT in the absence of stress-induced perfusion abnormalities. Eur J Nucl Med Mol Imaging. 2011;38:485–90.
40. Bravo PE, Pinheiro A, Higuchi T, Rischpler C, Merrill J, Santaularia-Tomas M, et al. PET/CT assessment of symptomatic individuals with obstructive and nonobstructive hypertrophic cardiomyopathy. J Nucl Med. 2012;53:407–14.
41. Cannon 3rd RO, Rosing DR, Maron BJ, Leon MB, Bonow RO, Watson RM, et al. Myocardial ischemia in patients with hypertrophic cardiomyopathy: contribution of inadequate vasodilator reserve and elevated left ventricular filling pressures. Circulation. 1985;71:234–43.
42. Gutiérrez-Barrios A, Camacho-Jurado F, Díaz-Retamino E, Gamaza-Chulián S, Agarrado-Luna A, Oneto-Otero J, et al. Invasive assessment of coronary microvascular dysfunction in hypertrophic cardiomyopathy: the index of microvascular resistance. Cardiovasc Revasc Med. 2015;16:426–8.
43. Raphael CE, Cooper R, Parker KH, Collinson J, Vassiliou V, Pennell DJ, et al. Mechanisms of Myocardial Ischemia in Hypertrophic Cardiomyopathy: Insights From Wave Intensity Analysis and Magnetic Resonance. J Am Coll Cardiol. 2016;68:1651–60.
44. Di Carli MF, Dorbala S, Meserve J, El Fakhri G, Sitek A, Moore SC. Clinical myocardial perfusion PET/CT. J Nucl Med. 2007;48:783–93.
45. Hickey KT, Sciacca RR, Bokhari S, Rodriguez O, Chou RL, Faber TL, et al. Assessment of cardiac wall motion and ejection fraction with gated PET using N-13 ammonia. Clin Nucl Med. 2004;29:243–8.
46. Peelukhana SV, Banerjee R, Kolli KK, Fernandez-Ulloa M, Arif I, Effat M, et al. Benefit of ECG-gated rest and stress N-13 cardiac PET imaging for quantification of LVEF in ischemic patients. Nucl Med Commun. 2015;36:986–98.
47. Klein R, Beanlands RS. deKemp RA. Quantification of myocardial blood flow and flow reserve: technical aspects. J Nucl Cardiol. 2010;17:555–70.
48. Le Meunier L, Slomka PJ, Dey D, Ramesh A, Thomson LE, Hayes SW, et al. Enhanced definition PET for cardiac imaging. J Nucl Cardiol. 2010;17:414–26.